Characterization of Zirconium−Silicon Binary Oxide Catalysts Prepared by the Sol−Gel Method and Their Photocatalytic Activity for the Isomerization of 2-Butene

Sang-Chul Moon, Mutsuko Fujino, Hiromi Yamashita, and Masakazu Anpo*

Department of Applied Chemistry, College of Engineering, Osaka Prefecture University, 1-1 Gakuen-cho, Sakai, Osaka 593, Japan

Received: May 24, 1996; In Final Form: August 23, 1996[⊗]

Zirconium−silicon binary oxide catalysts having different Zr concentrations were prepared by the sol−gel method and used as photocatalysts. The photocatalytic activity of these catalysts was investigated for the isomerization of *cis*-2-butene and was found to be enhanced in regions of lower Zr content. In situ photoluminescence, UV−vis reflectance, XRD, EXAFS, and XPS spectroscopic investigations of these zirconium−silicon oxide catalysts indicated that the Zr ions in the oxides which have a low Zr concentration exist separately as extremely small zirconium oxide species in the SiO_2 matrix while the radiative decay from the charge-transfer excited state of these species results in a characteristic photoluminescence. These results and the quenching of the photoluminescence by the added butene molecules showed that the higher photocatalytic activity of the zirconium−silicon binary oxides having a low Zr content is linked to the catalytic activity of the charge-transfer excited state of the zirconium oxide species, $[Zr^{3+}-O^{-}]$*, in the catalysts.

Introduction

ZrO_2 is well-known as an active catalyst for the hydrogenation of carbon monoxide to produce alcohol and isobutene. The reaction mechanism for the synthesis of alcohol and isobutene on ZrO_2 has been reported by Onishi et al.[1−5] and Ekerdt et al.[6−9] Tanabe et al. have also reported that ZrO_2 catalysts exhibit catalytic activity for the isomerization of 1-butene to *cis*- and *trans*-2-butenes at 373 K.[10] Furthermore, it has been established that coordinatively unsaturated surface sites are produced on the powdered oxides by evacuation at higher temperatures and that they not only play a significant role in the appearance of abnormal absorption and photoluminescence in insulating materials such as MgO and SrO but are also vital as active sites for catalytic reactions on these oxides.[11−14] We have observed the abnormal absorption and photoluminescence spectra with ZrO_2 catalysts degassed at temperatures higher than 600 K, suggesting that such coordinatively unsaturated surface sites which correspond to the abnormal absorption and photoluminescence are also formed on the powdered ZrO_2 catalysts by evacuation at higher temperatures. Furthermore, we have also observed that on these ZrO_2 catalysts, hydrogen molecules adsorb dissociatively and the hydrogenation of carbon monoxide and ethylene proceed effectively and efficiently.[15−17]

The sol−gel process offers unique advantages for the preparation of highly dispersed transparent catalysts, coating materials, active thin film photocatalysts, and multicomponent ceramics. Recently, Anthony et al. have reported that Zr/Si binary oxides prepared by the sol−gel method exhibit catalytic activity for the selective formation of isobutane and isobutene from synthesis gas.[18] Zr/Si binary oxides having strong acid sites have also been found to exhibit catalytic activity for the dehydrogenation of cyclohexanol.[19] Also, coordinatively unsaturated surface species on magnesium oxide particles are known to be generated on the Mg/SiO_2 oxides prepared by an impregnation method as well as to play a significant role in the photocatalytic oxidation reaction of propylene with O_2 on the catalyst.[20] However, until now there have been no investigations on the photocatalytic properties of zirconium−silicon binary oxide catalysts nor a clarification of the role of coordinatively unsaturated surface species on zirconium oxide particles.

In the present study, we deal with the characterization of zirconium−silicon binary oxide catalysts prepared by the sol−gel method by means of in situ photoluminescence, UV−vis reflectance, EXAFS, XPS, and XRD spectroscopic techniques and their photocatalytic activity for the isomerization of *cis*-2-butene into *trans*-2-butene and 1-butene at 295 K using a photocatalytic flow reaction system.

Experimental Section

Preparation of Catalysts. Zirconium−silicon (Zr/Si) binary oxides having different Zr contents were prepared by the sol−gel method from mixtures of tetraethyl orthosilicate (TEOS) and zirconium oxychloride in ethanol. The Zr/Si gels were obtained by keeping the mixture at room temperature for 3 days. The Zr/Si oxide gels formed in this way were washed with sufficient amounts of boiled water and then calcined in O_2 at 773 K for 5 h. The Zr/Si binary oxide samples were crushed and sieved to 0.25-mm-size particles. The ZrO_2 powdered catalysts were prepared by the precipitation of the $ZrO(NO_3)_2$ solution with NH_4OH after which the precipitates were dried and calcined in O_2 at 773 K. Prior to the spectroscopic measurements and photocatalytic reactions, the catalysts were evacuated for 5 h at the desired temperatures in the region of 300−1073 K.

Characterization. The photoluminescence spectra of the catalyst were measured at 295 and 77 K using a Shimadzu RF-5000 spectrophotofluorometer. The UV−vis reflectance spectra were measured at 295 K by a Shimadzu UV-2200A double-beam digital spectrophotometer equipped with conventional components of a reflectance spectrometer. X-ray diffraction patterns of the catalysts were obtained with a Rigaku RDA-γA X-ray diffractometer using Cu Kα radiation with a Ni filter. The XPS spectra were measured at 295 K with a V.G. Scientific ESCASCOPE photoelectron spectrometer using Mg Kα radiation. The X-ray absorption fine spectra of the Zr/Si binary oxide catalysts were obtained in the transmission mode using an EXAFS at the BL10B facility of the Photon Factory in the National Laboratory for High Energy Physics (KEK-PF), Tsukuba. A Si(311) channel-cut crystal was used to mono-

* To whom correspondence should be addressed.

[⊗] Abstract published in *Advance ACS Abstracts,* December 15, 1996.

S1089-5647(96)01523-4 CCC: $14.00

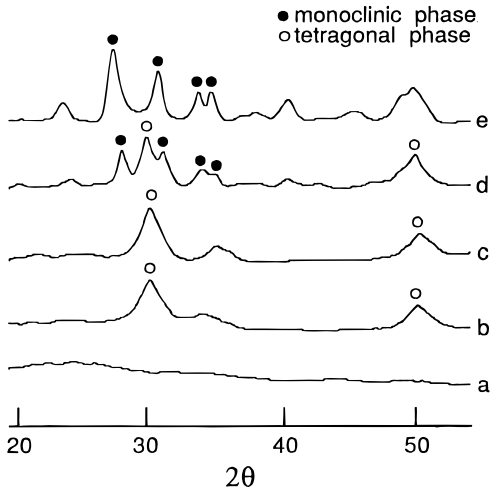

Figure 1. X-ray diffraction patterns of powdered ZrO_2 and Zr/Si binary oxides: (a) Zr/Si binary oxide of 17.0 wt % as ZrO_2 (Zr/Si = 0.19), (b) 45.1 wt % (Zr/Si = 0.4), (c) 55.2 wt % (Zr/Si = 0.6), (d) 67.2 wt % (Zr/Si = 1.0), and (e) powdered ZrO_2 catalyst.

chromatize the X-rays from the 2.5 GeV electron storage ring. The Fourier transformation was performed on the k^3-weighted EXAFS oscillation in the range of 3−12 $Å^{-1}$.

Photocatalysis. The photocatalytic isomerization of *cis*-2-butene was performed in a quartz tube cell connected to a flowing system. Prior to the photocatalytic reaction experimentation, the Zr/Si binary oxide catalysts were pretreated under the flow of 7 vol % O_2 in Ar at 573 K. The reactant gas flow of 0.3 vol % *cis*-2-butene in Ar was then introduced into the quartz tube reactor. UV-irradiation was carried out with a high-pressure Hg lamp (λ > 250 nm) at 295 K. The reaction products were collected at defined reaction intervals and analyzed by gas chromatography.

Results and Discussion

The crystalline structures of Zr/Si binary oxide catalysts having different Zr contents were investigated by XRD measurements. The XRD patterns obtained are shown in Figure 1. The crystalline structures of the Zr/Si binary oxides were different from that of ZrO_2 powders having a monoclinic phase and changed with the Zr content in the oxides. As shown in Figure 1, the X-ray patterns of the Zr/Si binary oxide catalysts show only the diffraction lines attributed to the two crystalline phases of ZrO_2, the monoclinic phase and the tetragonal phase. When the Zr content is decreased, the diffraction lines due to the monoclinic phase decreased in intensity, and simultaneously the diffraction lines due to the tetragonal phase of ZrO_2 appeared in the oxides having Zr contents lower than 67.2 wt % as ZrO_2. A further decrease in the Zr content led to the disappearance of the X-ray diffraction lines attributed to these monoclinic and tetragonal phases of ZrO_2. Such features indicate that in Zr/Si oxide catalysts, the crystallinity of the zirconium oxide species decreases dramatically and then disappears in the low Zr content region. Especially, in the Zr/Si binary oxide catalysts having Zr contents lower than 17.0 wt % as ZrO_2, zirconium oxide species are present in amorphous structures in the SiO_2 matrices.

Figure 2 shows the UV−vis reflectance spectra of the Zr/Si binary oxides. It is clear that with decreasing Zr content the absorption band of the binary oxides shifts remarkably toward shorter wavelengths. Similar studies were carried out on the Ti/Si and Ti/Al binary oxides having various compositions of Ti:Si and Ti:Al, and a considerable shift toward shorter wavelengths was observed for the absorption band of the highly dispersed titanium oxide species.[21−22] Therefore, it can be said

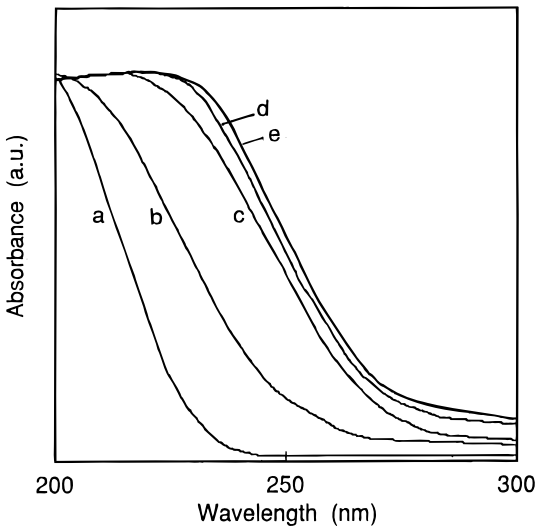

Figure 2. UV−vis reflectance spectra of Zr/Si binary oxides: (a) Zr/Si binary oxide of 3.9 wt % as ZrO_2 (Zr/Si = 0.02), (b) 9.3 wt % (Zr/Si = 0.05), (c) 45.1 wt % (Zr/Si = 0.4), (d) 67.2 wt % (Zr/Si = 1.0), and (e) powdered ZrO_2 catalyst.

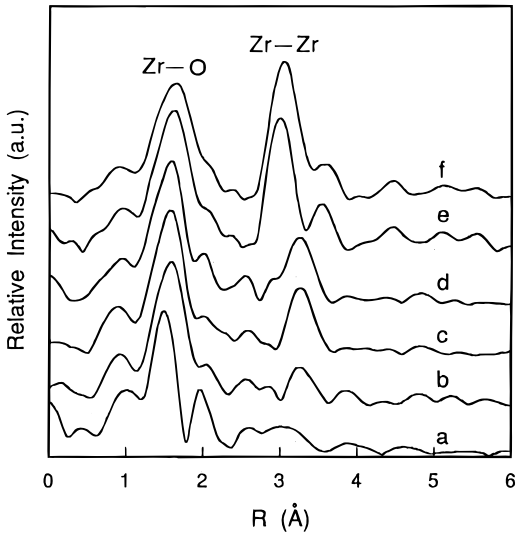

Figure 3. Fourier transforms of EXAFS spectra of powdered ZrO_2 catalyst and Zr/Si binary oxides: (a) Zr/Si binary oxide of 3.9 wt % as ZrO_2 (Zr/Si = 0.05), (b) 17.0 wt % (Zr/Si = 0.1), (c) 45.1 wt % (Zr/Si = 0.4), (d) 55.2 wt % (Zr/Si = 0.6), (e) 67.2 wt % (Zr/Si = 1.0), and (f) powdered ZrO_2 catalyst.

that such a large shift toward shorter wavelengths observed with the Zr/Si oxides having a low Zr concentration indicates the formation of ultrafine zirconium oxide species in the binary oxides, its extent strongly depending on the Zr content. These results obtained by XRD and UV−vis reflectance measurements clearly show that with decreasing Zr content in the Zr/Si binary oxide catalysts the crystalline structure of zirconium oxides changes from aggregates in a monoclinic phase to those in a tetragonal phase and then to ultrafine zirconium oxide species. These ultrafine zirconium oxide species have an amorphous structure in which the local coordinate geometry is different from those of the crystalline ZrO_2, as shown in the EXAFS studies (vide infra).

Figure 3a−e shows the Fourier transformation of the k^3-weighted EXAFS (FT-EXAFS) spectra of the Zr/Si binary oxide catalysts. Figure 3f shows the Fourier transformation of the ZrO_2 powders as a reference. As can be expected from the XRD studies, the FT-EXAFS spectra of the Zr/Si binary oxide catalysts with a high Zr content were similar to those of the

TABLE 1: Structure Parameters Determined from the Curve-Fitting Analysis of the EXAFS Spectra of the Zr/Si Binary Oxide Catalysts and the Powdered ZrO_2 Catalyst

sample	shell	coordination number	R/Å[a]
ZrO_2	Zr−O	7.0	2.20
Zr/Si binary oxide (Zr/Si = 1.0) (67.2 ZrO_2 wt %)	Zr−O	6.0	2.12
Zr/Si binary oxide (Zr/Si = 0.05) (9.3 ZrO_2 wt %)	Zr−O	4.5	2.05

[a] Bond distance.

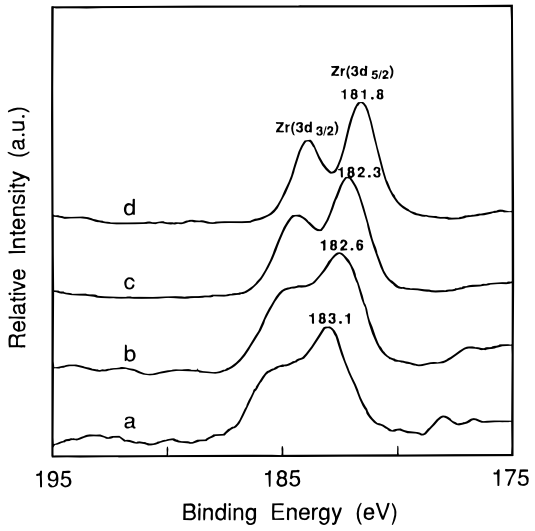

Figure 4. X-ray photoelectron spectra of the Zr ($3d_{3/2}$ and $3d_{5/2}$) level for the powdered ZrO_2 catalyst and Zr/Si binary oxides: (a) Zr/Si binary oxide of 9.3 wt % as ZrO_2 (Zr/Si = 0.05), (b) 17.0 wt % (Zr/Si = 0.1), (c) 55.2 wt % (Zr/Si = 0.6), and (d) powdered ZrO_2 catalyst.

ZrO_2 powder. The peak at around 1.6 Å in Figure 3 is assigned to the neighboring oxygen atoms (Zr−O), and this peak can clearly be observed with all Zr/Si binary oxides. However, as shown in Figure 3, it is clear that there is a steady decrease in the intensity of the peak at around 1.6 Å as the Zr content of the binary oxides decreases, indicating that the coordinatively unsaturated sites are formed on the zirconium oxide species. In fact, as shown in Table 1, the coordination numbers of the oxide determined from the curve-fitting analysis are found to change from 7 to 5 when the concentration of Zr in the oxides is decreased. On the other hand, the peak appearing at around 3.0 Å which is attributed to the neighboring Zr atoms (Zr−Zr) is observed only with Zr/Si binary oxides having Zr contents higher than 17.0 wt % as ZrO_2. These results indicate that zirconium oxide species are highly dispersed in Zr/Si binary oxides having lower Zr concentration and the aggregated ZrO_2 fine particles are formed in the SiO_2 matrices with increasing Zr content.

In order to obtain information on the binding energy of the zirconium oxide species in the Zr/Si binary oxides, the XPS spectra of the catalysts were measured. Figure 4a−c shows the XPS spectra of the Zr 3d band for the Zr/Si binary oxide catalysts having different Zr contents. The resolution of the peaks in the Zr($3d_{3/2}$) and Zr($3d_{5/2}$) XPS signals gradually becomes better as the Zr content increases and finally approaches the peaks of the powdered ZrO_2 catalyst when the Zr content reaches 55.2 wt % as ZrO_2. It can also be seen that the binding energy of the Zr($3d_{5/2}$) band shifts by 0.8 eV to a higher value with catalysts having less than 17.0 wt % as ZrO_2. A similar tendency has been observed for the Ti($2p_{3/2}$) XPS signals of the Ti/Si and Ti/Al binary oxides mentioned above. Considering these results, such a shift in the binding energy of the Zr($3d_{5/2}$) band to higher values can be attributed to the smaller relaxation energy for highly dispersed zirconium oxide species as compared to the powdered bulk ZrO_2 catalysts.

TABLE 2: Binding Energies of Zr($3d_{3/2}$), Zr($3d_{5/2}$), and Si($2p_{1/2}$) XPS Bands and the Ratio of the Signal Intensity of Zr($3d_{5/2}$) vs Si($2p_{1/2}$) in the Zr/Si Binary Oxides

	surface characterization			
sample Zr/Si binary oxide		binding energy (eV)		
	Zr($3d_{5/2}$)/Si($2p_{1/2}$)	Zr($3d_{3/2}$)	Zr($3d_{5/2}$)	Si($2p_{1/2}$)
pure ZrO_2	100% of ZrO_2	184.2	181.8	
Zr/Si = 0.6 (55.2 ZrO_2 wt %)	0.33	184.7	182.3	103.1
Zr/Si = 0.1 (17.0 wt %)	0.09	185.0	182.6	102.8
Zr/Si = 0.05 (9.3 wt %)	0.06	185.5	183.1	103.1
pure SiO_2	100% of SiO_2			104.0

Table 2 shows the ratio of the Zr($3d_{5/2}$) to Si($2p_{1/2}$) XPS band intensity. It is clear that there is a steady decrease in the intensity of Zr($3d_{5/2}$) signals as the Zr content in the Zr/Si binary oxides decreases. Furthermore, the ratio of the Zr($3d_{5/2}$) to Si($2p_{1/2}$) peak intensity is higher than what can be expected from the original composition of the sols in a lower content region of the Zr ion, suggesting the enrichment of Zr ions in the surface region of binary oxide catalysts having low Zr concentrations.

As has been reported in previous papers,[15−17] the ZrO_2 powders degassed at 1073 K exhibit a photoluminescence spectrum at around 500 nm upon excitation at around 285 nm. An abnormal absorption at around 285−300 nm and the photoluminescence at around 500 nm of the well-degassed ZrO_2 powders are attributed to the charge-transfer processes associated with coordinatively unsaturated surface sites in a manner similar to those for MgO and SrO powders:

$$(Zr^{4+}—O^{2-})_{LC} \underset{h\nu}{\overset{h\nu'}{\rightleftharpoons}} (Zr^{3+}—O^{-})^*_{LC} \qquad (1)$$

where LC = low coordination

In the present study, both Zr/Si binary oxides prepared by the sol−gel method and the Zr/SiO_2 catalyst prepared by an impregnation method exhibit photoluminescence spectra at around 430−480 nm when the absorption bond was excited at around 300 nm. These photoluminescence spectra are very similar to those of the powdered bulk ZrO_2 catalyst degassed at higher temperatures. However, as shown in Figure 5, the band positions of the photoluminescence of these Zr/Si binary oxides and Zr/SiO_2 catalysts can be observed at wavelengths much shorter than for those of the well-degassed ZrO_2 powders. The addition of oxygen onto the Zr/Si binary oxides leads to an efficient quenching of the photoluminescence, indicating that the emitting sites, i.e., $[Zr^{4+}—O^{2-}]_{LC}$ coordinatively unsaturated surface species, are present at the surface and/or near the surface regions to allow the added oxygen molecules access to the sites in a manner similar to those for various supported metal oxide catalysts.

Figure 6 shows the effect of the Zr content on the peak position and intensity of the photoluminescence spectrum due to the presence of highly dispersed zirconium oxide species in a state of coordinative unsaturation in the Zr/Si binary oxides. With decreasing Zr content, the intensity of the photoluminescence spectrum increases and the band position shifts to shorter wavelength regions. These findings indicate that decreasing the Zr content in the Zr/Si binary oxides causes the catalyst to exist in a highly dispersed state in the SiO_2 matrices with coordination numbers lower than those of ZrO_2 powders. Similar phenomena have been observed for the Ti/Si binary oxide catalysts prepared

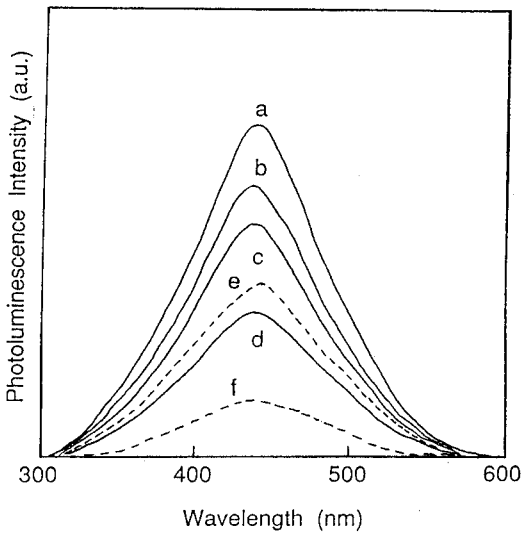

Figure 5. Effect of the addition of *cis*-2-butene or oxygen on the photoluminescence spectrum of the Zr/Si binary oxides (a). The amounts of added *cis*-2-butene (b) at 0.1 Torr, (c) at 1.0 Torr, and (d) at 10.0 Torr. The amounts of added oxygen (e) at 0.1 Torr and (f) at 1.0 Torr. (Photoluminescence spectra were recorded at 77 K. Addition of 2-butene or oxygen onto the catalysts was carried out at 295 K.)

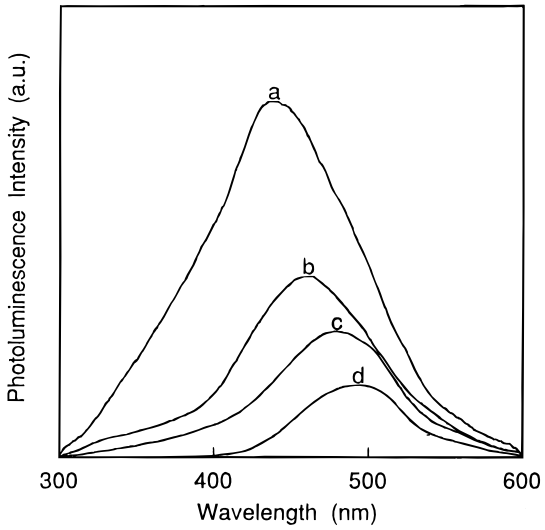

Figure 6. Photoluminescence spectrum of powdered ZrO_2 catalyst and Zr/Si binary oxides having different Zr contents at 77 K: (a) Zr/Si binary oxide of 9.3 wt % as ZrO_2 (Zr/Si = 0.05), (b) 17.0 wt % (Zr/Si = 0.1), (c) 55.2 wt % (Zr/Si = 0.6), and (d) powdered ZrO_2 catalyst.

by the sol−gel method; decreasing the Ti content in the Ti/Si binary oxides caused the photoluminescence intensity to increase, and its band position shifted to shorter wavelength regions, indicating that titanium oxide species are highly dispersed in the Ti/Si binary oxides.[23]

Figure 5 also shows the effect of the addition of *cis*-2-butene on the photoluminescence spectrum of the Zr/Si (Zr/Si = 0.02) binary oxide catalyst. Spectrum a was recorded after the evacuation of the oxide at 573 K. As shown in Figure 5b−d, the addition of *cis*-2-butene onto the Zr/Si binary oxide catalysts was found to lead to an efficient quenching of the photoluminescence, its extent strongly depending on the pressure of the added *cis*-2-butene. The addition of *cis*-2-butene (0.2 Torr) onto the Zr/Si binary oxide led to the shortening of the lifetime of the photoluminescence from 2.52 ns to 1.75 ns, its extent depending on the pressure of butene. These findings suggest that the charge-transfer excited state of the coordinatively unsaturated zirconium oxide species easily interacts with the added *cis*-2-butene.

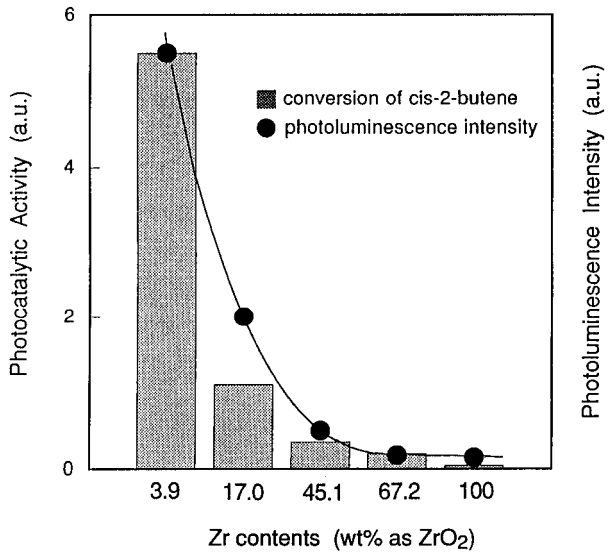

Figure 7. Relationship between the specific intensity of the photoluminescence of the Zr/Si binary oxide catalysts and the specific photocatalytic reactivities for the isomerization of *cis*-2-butene of these catalysts.

In fact, UV-irradiation of the Zr/Si binary oxides in the presence of *cis*-2-butene led to the photocatalytic isomerization of *cis*-2-butene to produce *trans*-2-butene (geometrical isomerization) as the major product and 1-butene (double-bond shift isomerization) as the minor product. After prolonged UV irradiation time, the number of the photoinduced isomerization products becomes larger than the number of Zr ions in the catalyst, indicating that the reaction proceeds photocatalytically at 298 K. At the reaction temperature, the thermal isomerization reaction scarcely proceeded and the reaction products were negligible as compared to the photocatalytic isomerization reactions.

It was also found that the photocatalytic activity of the Zr/Si binary oxide catalysts increased when the Zr content is decreased. As described above, the intensity of the photoluminescence of these catalysts attributed to the radiative decay from the charge-transfer excited state of the coordinatively unsaturated zirconium oxide species increased in regions of lower Zr content, and its peak position shifted to shorter wavelength regions indicating that the zirconium oxide species are highly dispersed in the SiO_2 matrices. Figure 7 shows the relationship between the specific photocatalytic activity per weight of the Zr/Si binary oxide catalysts for the isomerization of *cis*-2-butene and the specific photoluminescence yields per weight of the catalysts. The former was calculated from the conversions of butenes measured during the reaction period when the stable photocatalytic reactions proceeded steadily and constantly. As shown in Figure 7, the photocatalytic activity is in a good relationship with the photoluminescence yield of the catalysts, directly indicating that the charge-transfer excited state of the coordinatively unsaturated zirconium oxide species plays a significant role in the photocatalyzed isomerization reaction on the Zr/Si binary oxides.

From these results, it can be concluded that the interaction of *cis*-2-butene with the coordinatively unsaturated zirconium oxide species in their charge-transfer excited state occurs easily and the interaction of *cis*-2-butene with the charge-transfer excited state of the $[Zr^{3+}-O^-]^*$ paired state or the O^- species of the pair state of the zirconium oxide results in the opening of its C=C double bond which in turn results in the geometrical isomerization of *cis*-2-butene into *trans*-2-butene in a manner similar to that proposed for the photocatalytic isomerization of

2-butene on well-degassed MgO powders with coordinatively unsaturated surface sites.

Conclusions

Using the sol−gel technique, Zr−Si binary oxide catalysts having different Zr concentrations were prepared in a homogeneous structure. When the Zr concentration is decreased, the crystalline structure of the zirconium oxides in the Zr/Si binary oxide catalysts caused the structure to change from monoclinic to tetragonal and then to an amorphous state while a simultaneous enrichment of the Zr ions in the surface region was also observed. In the Zr/Si binary oxide having lower Zr content, the ultrafine zirconium oxide species were found to exist separately from each other in the SiO_2 matrices and exhibited a typical photoluminescence spectrum attributed to the radiative decay from the charge-transfer excited state of these species. The efficient quenching of the photoluminescence with the addition of *cis*-2-butene indicated the interaction of butene with the charge-transfer excited state of the coordinatively unsaturated surface sites of the zirconium oxide species, i.e., $[Zr^{3}-O^{-}]^{*}$. These ultrafine zirconium oxide species in the Zr/Si binary oxide exhibited a specific photocatalytic activity for the isomerization of *cis*-2-butene. The good parallelism between the photoluminescence yield and the photocatalytic activity obtained with the Zr/Si binary oxide catalysts having different Zr contents clearly indicated that the charge-transfer excited state of the emitting sites of the zirconium oxide species plays a significant role in the photocatalytic isomerization of *cis*-2-butene on the catalysts.

References and Notes

(1) Abe, H.; Maruya, K. I.; Domen, K.; Onishi, T. *Chem. Lett.* **1984**, 1875.

(2) Maruya, K. I.; Inabe, A.; Maehashi, T.; Domen, K.; Onishi, T. *J. Chem. Soc., Chem. Commun.* **1985**, 487.

(3) Kondo, J.; Abe, H.; Sakata, Y.; Maruya, K. I.; Domen, K.; Onishi, T. *J. Chem. Soc., Faraday Trans. 1* **1988**, *84*, 511.

(4) Maruya, K. I.; Maehashi, T.; Haraoka, T.; Narui, S.; Asakawa, Y.; Domen, K.; Onishi, T. *Bull. Chem. Soc. Jpn.* **1988**, *61*, 667.

(5) Maruya, K. I.; Fujisawa, T.; Takasawa, A.; Domen, K.; Onishi, T. *Bull. Chem. Soc. Jpn.* **1989**, *62*, 11.

(6) He, M. Y.; Ekerdt, J. G. *J. Catal.* **1984**, *87*, 238.

(7) He, M. Y.; Ekerdt, J. G. *J. Catal.* **1984**, *87*, 381.

(8) Jackson, N. B.; Ekerdt, J. G. *J. Catal.* **1986**, *101*, 90.

(9) Tseng, S. C.; Jackson, N. B.; Ekerdt, J. G. *J. Catal.* **1988**, *109*, 284.

(10) Yamaguchi, T.; Sakai, H.; Tanabe, K. *Chem. Lett.* **1973**, 1017.

(11) Anpo, M.; Yamada, Y.; Kubokawa, Y. *J. Chem. Soc., Chem. Commun.* **1986**, 714.

(12) Anpo, M.; Yamada, Y. *Shokubai (Catalysis)* **1987**, *29*, 470.

(13) Anpo, M.; Yamada, Y.; Kubokawa, Y.; Coluccia, S.; Zecchina, A.; Che, M. *J. Chem. Soc., Faraday Trans. 1* **1988**, *84*, 751.

(14) Anpo, M.; Moon, S. C.; Chiba, K.; Martra's, G.; Coluccia, S. *Res. Chem. Intermed.* **1993**, *19*, 495.

(15) Anpo, M.; Nomura, T.; Kondo, J.; Maruya, K. I.; Onishi, T. *Res. Chem. Intermed.* **1990**, *13*, 195.

(16) Moon, S. C.; Yamashita, H.; Anpo, M. *Acid-Base Catalysis II*; Hattori, H., Misono, M., Ono, Y., Eds.; Kodansha: Tokyo, 1994; pp 479−484.

(17) Moon, S. C.; Tsuji, K.; Nomura, T.; Anpo, M. *Chem. Lett.* **1994**, 2241.

(18) Feng, Z.; Postula, W. S.; Erkey, C.; Philip, C. V.; Akgerman, A.; Anthony, R. G. *J. Catal.* **1994**, *148*, 84.

(19) Bosman, H. J. M.; Kruissink, E. C.; van der Spoel, J.; van den Brink, F. *J. Catal.* **1994**, *148*, 660.

(20) Tanaka, T.; Yoshida, H.; Nakatsuka, K.; Funabiki, T.; Yoshida, S. *J. Chem. Soc., Faraday Trans.* **1992**, *88*, 2297.

(21) Anpo, M.; Nakaya, H.; Kodama, S.; Kubokawa, Y.; Domen, K.; Onishi, T. *J. Phys. Chem.* **1986**, *90*, 1633.

(22) Anpo, M.; Kawamura, T.; Kodama, S. *J. Phys. Chem.* **1988**, *92*, 438.

(23) Yamashita, H.; Kawasaki, S. I.; Anpo, M.; Stewart, G.; Fox, M. A.; Arendt, M. F.; White, J. M. In *Abstracts of International Conference on Photochemical Conversion & Storage of Solar Energy (ISP-10)*; Calzaferri, G., Ed.; Interaken, Switzerland, 1994; p 403.